diaminobenzidine (DAB)–based reaction with Ni/Co-enhanced antibody to BrdU as described above, combined with a standard, nonenhanced reaction revealing the cell type. The double-staining for donor-derived astrocytes (colocalization of BrdU and GFAP) followed a similar protocol with a rabbit polyclonal antibody to GFAP (Daco) but with the two secondary antibodies (Vector Labs) coupled to different fluorochromes: fluorescein to reveal BrdU and Texas Red for GFAP. As noted above, we used multiple independent markers to show unambiguously donor derivation of the examined cells; the labeling distribution for each of the markers was the same.

29. G. D. Frantz, S. K. McConnell, *Neuron* **17**, 55 (1996).
30. S. A. Goldman, M. B. Luskin, *Trends Neurosci.* **21**, 107 (1998).
31. A. Kakita, J. E. Goldman, *Neuron* **23**, 461 (1999).
32. E. Gould, A. J. Reeves, M. S. Graziano, C. G. Gross, *Science* **286**, 548 (1999).
33. S. S. Magavi, B. R. Leavitt, J. D. Macklis, *Nature* **405**, 951 (2000).
34. K. I. Park, E. Y. Snyder, *Soc. Neurosci. Abstr.* **24**, 1310 (1998).
35. M. F. Mehler, S. Gokhan, *Brain Pathol.* **9**, 515 (1999).
36. R. L. Sidman, P. Rakic, in *Histology and Histopathology of the Nervous System*, W. Haymaker, R. D. Adams, Eds. (Thomas, Springfield, MA, 1982), pp. 3–145.
37. An evaluation of surviving grafted cells in all three animals revealed ~150 to 200 cells per 35-μm coronal section in the most densely engrafted areas (usually at level I; see Fig. 2) and ~10 cells per section in the more sparsely engrafted regions. Whether this distribution reflects a genuine anterior-posterior developmental gradient or simply a stochastic distribution of cells or the product of transplantation technique cannot yet be determined. An estimate of ~10^5 hNSC-derived cells were detectable per monkey brain. hNSCs segregated in about a 3:7 ratio proportion between subpopulation 1 and subpopulation 2, respectively. Of subpopulation 1 cells in the cortex, 7 to 8% were neurons, 80% were astrocytes, and 12% were oligodendrocytes; the neurons were almost invariantly in the appropriate laminae II and III.
38. Two of the three pregnant monkeys received cyclosporin, as described in (*23*). No histological evidence of inflammatory reaction or of cell rejection was seen in any of the three specimens. Experiments of longer duration and with grafting at more mature ages will be necessary to test whether rejection might ultimately have occurred; however, there is the suggestion that, at least at certain stages, an immunotolerance for NSCs might exist.
39. V. Ourednik, J. Ourednik, K. I. Park, E. Y. Snyder, *Clin. Genet.* **56**, 267 (1999).
40. Funded by National Institute of Neurological Disorders and Stroke, March of Dimes, Project ALS, A-T Children's Project, Mental Illness Research Association, Kingspoint Richmond Foundation, Conavan Research Fund, Hunter's Hope, International Organization for Glutaric Acidemia, a Mental Retardation Research Center Grant to Children's Hospital, Program to End Parkinson's Disease, and Parkinson's Action Network.

9 March 2001; accepted 16 July 2001
Published online 26 July 2001;
10.1126/science.1060580
Include this information when citing this paper.

Allele-Specific Receptor-Ligand Interactions in *Brassica* Self-Incompatibility

Aardra Kachroo, Christel R. Schopfer,* Mikhail E. Nasrallah, June B. Nasrallah†

Genetic self-incompatibility in *Brassica* is determined by alleles of the transmembrane serine-threonine kinase SRK, which functions in the stigma epidermis, and of the cysteine-rich peptide SCR, which functions in pollen. Using tagged versions of SRK and SCR as well as endogenous stigma and pollen proteins, we show that SCR binds the SRK ectodomain and that this binding is allele specific. Thus, SRK and SCR function as a receptor-ligand pair in the recognition of self pollen. Specificity in the self-incompatibility response derives from allele-specific formation of SRK-SCR complexes at the pollen-stigma interface.

In self-incompatible *Brassica* plants, self-pollinations and crosses between genetically related individuals are nonproductive because self-related pollen grains are inhibited upon contact with the epidermal cells of the stigma, a structure that caps the female reproductive organ. Specificity in this self-incompatibility (SI) response is determined by haplotypes of the polymorphic *S* locus. The self-recognition molecules encoded by this locus include the single-pass transmembrane receptor–like serine-threonine kinase SRK, which functions in the stigma epidermis (*1–3*) and becomes phosphorylated upon self-pollination (*4*), and the cysteine-rich peptide SCR, which functions in pollen (*5*, *6*). These two molecules are highly polymorphic, with allelic forms of SRK and SCR exhibiting 10 to 30% and >60% divergence, respectively (*1*, *5–8*). Views of SRK as a ligand-activated receptor kinase and SCR as its ligand are consistent with the predicted molecular properties of these molecules and the rapidity of the SI response (*1*, *9*). The SCR peptide is localized on the surface of pollen grains (*10*). During self-pollination, SCR is predicted to bind the receptor domain of its cognate SRK, thereby triggering an intracellular phosphorylation cascade that leads to inhibition of pollen hydration and germination. Specificity in the SI response is thought to result from haplotype-specific activation of SRK by SCR. Here, we describe experiments that demonstrate a physical and haplotype-specific interaction between SCR and the ectodomain of SRK.

To investigate the SRK-SCR interaction, we generated tagged versions of the two proteins. Recombinant $eSRK_6$, consisting of the ectodomain of SRK_6 (from the S_6 haplotype) and carrying a COOH-terminal FLAG epitope tag, was expressed as a soluble secreted glycoprotein in *Nicotiana benthamiana* leaves using the potato virus X expression system (*11*). $eSRK_6$ protein migrated as two molecular mass forms of ~63 and 70 kD on SDS–polyacrylamide gel electrophoresis (SDS-PAGE), which presumably reflect differential glycosylation of $eSRK_6$-FLAG in *Nicotiana* leaves. SCR_6 and SCR_{13} (the SCRs of the S_6 and S_{13} haplotypes, respectively) were expressed in bacteria as secreted periplasmic proteins carrying a COOH-terminal myc-His_6 tag (*11*). They exhibited expected masses of ~8 and 9 kD, respectively, but they migrated as doublets, possibly due to inefficient cleavage of the periplasmic signal peptide in bacteria.

Recombinant SCR-myc-His_6 was shown to be biologically active in pollination bioassays (*12*). Pretreatment of stigmas with purified "self" SCR protein (i.e., S_6S_6 stigmas with SCR_6-myc-His_6 or $S_{13}S_{13}$ stigmas with SCR_{13}-myc-His_6) mixed with pollen-coat protein carrier (*12*) caused these stigmas to inhibit the germination of normally compati-

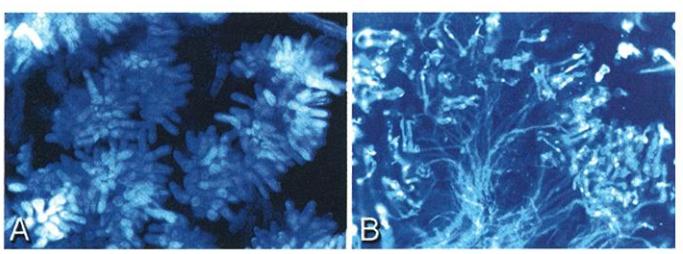

Fig. 1. Effect of purified recombinant SCR protein on cross-pollen tube development. S_6S_6 stigmas (**A**) and S_2S_2 stigmas (**B**) were treated with SCR_6-myc-His_6 and pollinated with S_{13} pollen (*12*). Addition of "self" SCR_6-myc-His_6 triggers inhibition of normally compatible S_{13} pollen on S_6S_6 but not on S_2S_2 stigmas.

Department of Plant Biology, Cornell University, Ithaca, NY 14853, USA.

*Present Address: SunGene GmbH, Correnssstrasse 3, D-06466, Gatersleben, Germany.
†To whom correspondence should be addressed. E-mail: jnb2@cornell.edu

ble "non-self" pollen (Table 1, Fig. 1A). In contrast, "non-self" pollen could develop on stigmas treated with "non-self" SCR protein (e.g., S_6S_6 stigmas treated with SCR_{13}-myc-His_6) (Table 1, Fig. 1B). Thus, recombinant SCR-myc-His_6 activates the SI response specifically in stigmas that express the cognate SRK.

SRK and SCR were shown to interact in vitro by "pull-down" assays (Fig. 2A) in which $eSRK_6$ immobilized on FLAG-affinity agarose was treated with increasing amounts of SCR_6-myc-His_6, and the complexes were subjected to immunoblot analysis (*13*). In addition, an enzyme-linked immunosorbent assay (ELISA) (*14*) showed that $eSRK_6$ bound SCR_6 in a concentration-dependent manner (Fig. 2B), with a dissociation constant (K_d) of 0.4×10^{-10} M. In contrast, $eSRK_6$ bound poorly to SCR_{13}, even at high concentrations of SCR_{13}-myc-His_6 (Fig. 2B). The ~10-fold stronger binding of $eSRK_6$ to self SCR_6 than to non-self SCR_{13} demonstrates the specificity of the in vitro SRK-SCR interaction and provides a molecular basis for haplotype-specificity in the SI response.

To assess whether $eSRK_6$ also bound endogenous SCR_6 from pollen, pollen coat proteins were extracted from S_6 pollen (*15*) and incubated with $eSRK_6$ beads, and the resulting complexes were subjected to electrophoresis under nonreducing conditions (*13*). Under these conditions, purified SCR_6-myc-His_6 molecules migrated as a ~16-kD band, likely consisting of homodimers, with only a small fraction migrating as monomers (Fig. 2C, lane 1). The antibodies to SCR_6 also reacted with ~16-kD molecules in pollen coat extracts (Fig. 2C, lane 2), and these cross-reactive molecules were bound by $eSRK_6$ in a concentration-dependent manner (Fig. 2C, lanes 4 through 9). It is not known whether these SCR homodimers represent the native state of SCR in pollen and whether homodimerization is required for the binding of the SCR to SRK in vivo. These experiments demonstrate that the SRK ectodomain interacts with endogenous pollen SCR and provide biochemical evidence that SCR is a component of the pollen coat, as suggested by the expression pattern of the *SCR* gene (*5*, *6*, *16*) and the immunolocalization of SCR to the pollen surface (*10*).

The SRK-SCR interaction was confirmed by reversing the pull-down assay. Recombinant SCR_6 immobilized on Ni-agarose beads bound $eSRK_6$ from *N. benthamiana* leaves (Fig. 2D). Furthermore, these SCR_6 beads bound endogenous SRK_6 in S_6S_6 stigma microsomal fractions (*17*, *18*) but did not bind SRK_{13} from $S_{13}S_{13}$ stigma microsomes (Fig. 2D). Similarly, recombinant SCR_{13} immobilized on Ni-agarose beads bound to stigma SRK_{13} but not to SRK_6. Thus, according to our in vitro binding assays, SCR can discriminate between allelic forms of SRK that share a substantial amount (~90%) of amino acid sequence identity. The SCR_6 beads also bound—albeit poorly—to SLG_6, an abundant glycoprotein component of the cell wall of stigma epidermal cells that exhibits 89% sequence identity with the SRK_6 ectodomain and, like SRK, is encoded by the *S* locus and exhib-

Table 1. Inhibition of normally cross-compatible pollen on stigmas pretreated with self recombinant SCR protein. Purified SCR-myc-His_6 proteins were added to the stigma before pollination (*12*), except where indicated by (–). In the Pollen coat protein column, "+" indicates that pollen coat protein was added as carrier; "–" indicates that no pollen coat protein was added. Pollen tube development data represent absence (no) or presence (yes) of pollen tubes. Experimental treatments used two different SCR protein preparations and were done in four independent trials, each consisting of two to four pollinated stigmas.

Stigma genotype	Purified recombinant SCR	Pollen coat protein	Pollen	Pollen tube development
S_6S_6	SCR_6	+	S_{13}, S_2, or S_{22}	no
S_6S_6	SCR_{13}	+	S_{13}, S_2, or S_{22}	yes
S_6S_6	–	+	S_{13}, S_2, or S_{22}	yes
S_6S_6	–	–	S_{13}, S_2, or S_{22}	yes
S_6S_6	–	–	S_6	no
$S_{13}S_{13}$	SCR_{13}	+	S_6, S_2, or S_{22}	no
$S_{13}S_{13}$	SCR_6	+	S_6, S_2, or S_{22}	yes
$S_{13}S_{13}$	–	+	S_6, S_2, or S_{22}	yes
$S_{13}S_{13}$	–	–	S_6, S_2, or S_{22}	yes
$S_{13}S_{13}$	–	–	S_{13}	no
S_2S_2	SCR_6	+	S_6 or S_{13}	yes
S_2S_2	SCR_{13}	+	S_6 or S_{13}	yes
S_2S_2	–	+	S_6 or S_{13}	yes
S_2S_2	–	–	S_6 or S_{13}	yes

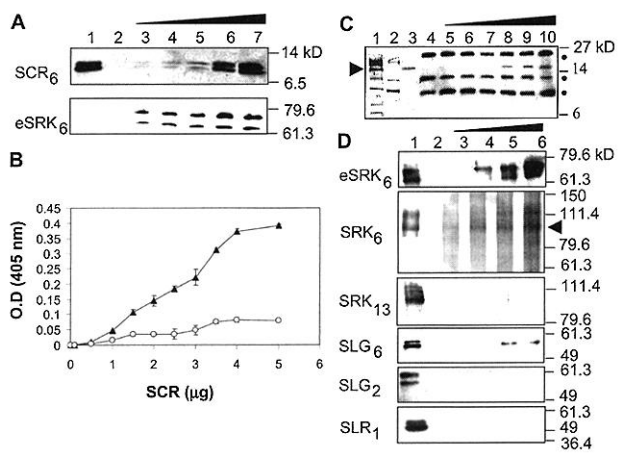

Fig. 2. Binding of SCR to the SRK ectodomain. (**A**) Protein blot analysis of the interaction between $eSRK_6$-FLAG and SCR_6-myc-His_6. $eSRK_6$-FLAG (750 ng) immobilized on affinity agarose was incubated with increasing amounts of SCR_6-myc-His_6 [50 ng (lane 3), 100 ng (lane 4), 500 ng (lane 5), 1 μg (lane 6), and 2 μg (lane 7)]. Immunoblots of bead-protein complexes were treated with antibodies to myc (top panel) to detect bound SCR or with MabH8 (lower panel) to confirm that all bead complexes contained equivalent amounts of $eSRK_6$-FLAG. SCR_6-myc-His_6 (1 μg), used as positive control (lane 1), did not bind anti-FLAG agarose (lane 2). (**B**) ELISA of SRK-SCR binding. $eSRK_6$-FLAG (0.5 μg) exhibited high affinity for SCR_6-myc-His_6 (triangles) but weak affinity for SCR_{13}-myc-His_6 (circles). Values represent an average of three experiments. (**C**) Interaction of $eSRK_6$-FLAG with pollen SCR_6. $eSRK_6$-FLAG-agarose was incubated with S_6 pollen coat proteins and subjected to nonreducing SDS-PAGE (*13*). Anti-SCR_6 serum detects SCR_6 as an ~16-kD band (arrowhead) and two minor 6- to 8-kD bands that probably correspond to SCR monomers in bacterial extracts (lane 1) and as an ~16-kD band in pollen coat protein extracts (lane 3). The serum also cross-reacts nonspecifically with several bacterial proteins that are also detected with preimmune serum (lane 2) and with three background bands (circles) in FLAG-agarose lacking $eSRK_6$ (lane 4). Incubation of $eSRK_6$-FLAG-agarose with increasing amounts of S_6 pollen coat protein [50 ng (lane 4), 100 ng (lane 5), 500 ng (lane 6), 1 μg (lane 7), 2 μg (lane 8), and 5 μg (lane 9)] demonstrates concentration-dependent binding of SCR_6 above the background of nonspecific cross-reactive bands. (**D**) SCR_6-myc-His_6 pull-down assays. SCR_6-myc-His_6 was immobilized on Ni-NTA agarose and incubated with increasing amounts of either $eSRK_6$-FLAG ($eSRK_6$), microsomal extracts from S_6S_6 (SRK_6) and $S_{13}S_{13}$ (SRK_{13}) stigmas, or soluble extracts from S_6S_6 (SLG_6) and S_2S_2 (SLG_2 and SLR1) stigmas. Untreated $eSRK_6$-FLAG (250 ng) served as positive control (lane 1), and untreated stigma proteins, which did not bind Ni-NTA agarose, served as negative control (lane 2). The amounts of $eSRK_6$-FLAG used were 50 ng (lane 3), 100 ng (lane 4), 250 ng (lane 5), and 500 ng (lane 6). The amounts of stigma microsomal or soluble proteins used were 250 ng (lane 3), 500 ng (lane 4), 1 μg (lane 5), and 2 μg (lane 6). Bound proteins were visualized with specific antibodies (*13*). The two bands in S_6S_6 stigma microsomal fractions that bind SCR_6-myc-His_6 represent SRK_6 (lower band, arrowhead), and SLG_6 oligomers (upper band) often detected in stigma extracts (*18*).

its extensive *S* haplotype-associated polymorphism (*19*, *20*). SLG has been shown to migrate on SDS-PAGE as a cluster of molecular mass forms (Fig. 2D) (*21*). However, only one of these SLG_6 forms bound to SCR_6 beads, suggesting a degree of specificity in the observed SLG_6-SCR_6 binding. Additional evidence for specificity is provided by the finding that treatment of S_2S_2 stigma extracts with SCR_6 beads failed to pull down detectable levels of SLG_2 or of the *S*-locus related *SLR1* and *SLR2* gene products (Fig. 2D), all of which exhibit only 65% amino acid sequence identity to SLG_6. SLG is thought to function, at least in some cases, as an accessory molecule that enhances the SRK-mediated SI response (*3*), possibly by contributing to the stabilization and proper maturation of SRK (*18*). The interaction observed between SCR and SLG suggests that some forms of SLG might also function in ligand binding. However, the physiological importance of this relatively weak interaction remains to be determined.

Our results demonstrate that SCR interacts with the ectodomain of SRK. Apparently, the SRK-SCR interaction does not require additional components specific to the stigma and pollen surfaces, because the interaction was observed between recombinant proteins purified from *Nicotiana* leaves and bacteria. The data indicate that specificity in the SI response results from *S* haplotype-specific molecular interaction of SCR and SRK, which would selectively trigger activation of self SRK and a pollen-inhibitory chain of events. Analysis of receptor-ligand interactions demonstrated by SRK-SCR and by CLV1-CLV3 of *Arabidopsis thaliana* (*22*) should provide useful paradigms for the study of transmembrane receptor signaling and of the function and regulation of small diffusible peptide ligands in plants.

References and Notes

1. J. C. Stein, B. H. Howlett, D. C. Boyes, M. E. Nasrallah, J. B. Nasrallah, *Proc. Natl. Acad. Sci. U.S.A.* **88**, 8816 (1991).
2. J. A. Conner *et al.*, *Plant J.* **11**, 809 (1997).
3. T. Takasaki *et al.*, *Nature* **403**, 913 (2000).
4. D. Cabrillac, J. M. Cock, C. Dumas, T. Gaude, *Nature* **410**, 220 (2001).
5. C. R. Schopfer, M. E. Nasrallah, J. B. Nasrallah, *Science* **286**, 1697 (1999).
6. SCR is designated SP-11 by S. Takayama *et al.* in [*Proc. Natl. Acad. Sci. U.S.A.* **97**, 1920 (2000)].
7. M. Kusaba, T. Nishio, *Plant J.* **17**, 83 (1999).
8. M. A. Watanabe *et al.*, *FEBS Lett.* **473**, 139 (2000).
9. J. B. Nasrallah, *Curr. Opin. Plant. Biol.* **3**, 368 (2000).
10. H. Shiba *et al.*, *Plant Phys.* **125**, 2095 (2001).
11. The SRK_6 ectodomain carrying a COOH-terminal FLAG epitope was cloned into the Potato Virus X (PVX)-derived vector pP2C2S′ (*23*). In vitro transcripts produced with the RiboMAX system (Promega, Madison, WI) were used to infect 4-week-old *N. benthamiana* plants. Infected leaves showing disease symptoms were ground in liquid nitrogen, resuspended in buffer [30 mM Tris-HCl pH 7.5, 75 mM NaCl, 10% v/v glycerol, 5 mM ascorbate, 2.5 mM potassium metabisulfite, 1 mM phenylmethylsulfonyl fluoride (PMSF), aprotinin (10 μg/ml), leupeptin (10 μg/ml), and pepstatin A (1 μg/ml)], and then $eSRK_6$-FLAG was purified on FLAG M2 affinity gel (Sigma, St. Louis, MO). Recombinant SCR_6 and SCR_{13} (without the signal peptide) carrying a COOH-terminal myc-His_6 were produced using the pBAD/gIIIB vector (Invitrogen, Carlsbad, CA) and were purified on Ni–nitriloacetic acid (Ni-NTA) affinity agarose (Qiagen, Valencia, CA).
12. Recombinant SCR proteins were assayed on stigmas collected from *S*-locus homozygotes, which are generated by manual pollination in immature buds before the developing buds acquire the ability to reject self-pollen. For these bioassays, which were modified from (*24*), carrier pollen coat protein (50 ng) was extracted with cyclohexane (*15*) from pollen that is genetically unrelated to the stigmas and pollen used for pollination, mixed with 300 ng of SCR_6-myc-His_6 or SCR_{13}-myc-His_6, and applied to S_6S_6 or $S_{13}S_{13}$ stigmas. Preliminary experiments showed that 300 and 60 ng of SCR applied to a stigma activated the incompatibility response and 30 ng were partially effective, whereas 3 ng and 0.6 ng were ineffective. Treated stigmas were allowed to dry for ~1 hour before pollination, and pollen tube growth was visualized by ultraviolet fluorescence microscopy (*5*). Controls included untreated stigmas, S_6S_6 and $S_{13}S_{13}$ stigmas treated with carrier pollen coat protein alone or with non-self SCR, and S_2S_2 stigmas treated with carrier pollen coat protein and the preparation of SCR used in the experimental samples.
13. SCR proteins were resolved on 15% SDS-PAGE and detected with antibodies to myc (Invitrogen). For detection with antibodies to SCR_6 generated against SCR_6–glutathione *S* transferase (SCR_6-GST) fusion proteins, reducing agents were omitted because they quenched antibody binding. $eSRK_6$ and stigma proteins were resolved on 7.5% SDS-PAGE and detected with antibodies to S domain: monoclonal MabH8, which detects SRK_6, SRK_{13}, SLG_6, and SLG_{13} (*17*, *18*); polyclonal antibodies to SLR2, which detect SLR2 and SLG_2 (*25*); and SLR1-specific polyclonal antibodies (*21*). Protein bands were visualized with horseradish peroxidase–conjugated secondary antibodies (Sigma) and the ECL+ system (Amersham Pharmacia Biotech, Piscataway, NJ).
14. ELISA was carried out according to (*26*). Microtiter plate wells were coated with 0.5 μg of $eSRK_6$ and then were incubated with increasing amounts of SCR_6-myc-His_6 or SCR_{13}-myc-His_6. After incubation with antibodies to myc and alkaline phosphatase–conjugated secondary antibody (Sigma), the reaction was developed with 100 μl of Sigma Fast pNPP substrate (Sigma), and absorbance was measured at 405 nm in an ELISA plate reader.
15. J. Doughty, F. Hedderson, A. McCubbin, H. G. Dickinson, *Proc. Natl. Acad. Sci. U.S.A.* **90**, 467 (1993).
16. C. R. Schopfer, J. B. Nasrallah, *Plant Physiol.* **124**, 935 (2000).
17. J. C. Stein, R. Dixit, M. E. Nasrallah, J. B. Nasrallah, *Plant Cell* **8**, 429 (1996).
18. R. Dixit, M. E. Nasrallah, J. B. Nasrallah, *Plant Physiol.* **124**, 297 (2000).
19. J. Nasrallah, T. H. Kao, C. H. Chen, M. L. Goldberg, M. E. Nasrallah, *Nature* **326**, 617 (1987).
20. M. Kusaba, T. Nishio, Y. Satta, K. Hinata, D. J. Ockendon, *Proc. Natl. Acad. Sci. U.S.A.* **94**, 7673 (1997).
21. A. L. Umbach, B. A. Lalonde, M. K. Kandasamy, J. B. Nasrallah, M. E. Nasrallah, *Plant Physiol.* **93**, 739 (1991).
22. A. E. Trotochaud, S. Jeong, S. E. Clark, *Science* **289**, 613 (2000).
23. D. C. Baulcombe, S. Chapman, S. Santa Cruz, *Plant J.* **7**, 1045 (1995).
24. A. G. Stephenson *et al.*, *Plant J.* **12**, 1351 (1997).
25. T. Tantikanjana, M. E. Nasrallah, J. B. Nasrallah, *Sex. Plant Reprod.* **9**, 107 (1996)
26. Y.-B. Lu, P. Ratnakar, B. K. Mohanty, D. Bastia, *Proc. Natl. Acad. Sci. U.S.A.* **93**, 12902 (1996).

27. We thank D. Baulcombe for the PVX vector, G. Martin and X. He for advice on PVX expression, D. Navarre for useful discussions, and T. Setter for help with ELISA. Supported by NIH grant GM57527.

14 May 2001; accepted 18 July 2001

Resistance to an Herbivore Through Engineered Cyanogenic Glucoside Synthesis

David B. Tattersall,[1,2] Søren Bak,[1,2]* Patrik R. Jones,[1,2,4]* Carl Erik Olsen,[2,3] Jens K. Nielsen,[3] Mads L. Hansen,[3] Peter B. Høj,[4,5] Birger Lindberg Møller[1,2]†

The entire pathway for synthesis of the tyrosine-derived cyanogenic glucoside dhurrin has been transferred from *Sorghum bicolor* to *Arabidopsis thaliana*. Here, we document that genetically engineered plants are able to synthesize and store large amounts of new natural products. The presence of dhurrin in the transgenic *A. thaliana* plants confers resistance to the flea beetle *Phyllotreta nemorum*, which is a natural pest of other members of the crucifer group, demonstrating the potential utility of cyanogenic glucosides in plant defense.

Cyanogenic glucosides are a group of amino acid–derived secondary metabolites that are widely distributed in the plant kingdom (*1*, *2*). When the plant tissue is disrupted by herbivore attack, the cyanogenic glucosides are degraded into a sugar, a keto compound, and hydrogen cyanide (HCN). This cyanogenesis confers protection against some, but not all, herbivore attacks (*1*, *3*). Insects feeding on cyanogenic plants may have evolved mechanisms to detoxify or to sequester cyanogenic glucosides (*4*–*6*), which in turn protect the insect against predators (*7*). To assess the effect of cyanogenesis, it is necessary to study insects that have not coevolved with cyanogenic glucosides. Such insects are found among those that specifically feed on cruciferous plants, which do not produce cyanogenic glucosides. To render investigations in such an experimental system possible, we transferred the pathway for cyanogenic glucoside biosynthesis into the cruciferous plant